Nematic order in suspensions of colloidal rods by application of a centrifugal field

Deshpremy Mukhija and Michael J. Solomon*

Received 9th June 2010, Accepted 4th October 2010
DOI: 10.1039/c0sm00493f

An applied field generated by centrifugation induced nematic order in colloidal rods of aspect ratio, r, varying from 3.6 to 8. The dependence of the order parameter, S, on dimensionless applied field strength was quantified by identifying the directors of the micron-sized poly(methyl methacrylate) rods in the suspension with confocal microscopy. The influence of the centrifugal field on orientational order was highly aspect ratio dependent. Order increased with field strength for $r = 3.6$, while it decreased with field strength for $r = 8.0$. All the measurements, however, were well correlated by ϕ/ϕ_{nem}, where ϕ_{nem} is the volume fraction of the nematic phase boundary. The most significant ordering of the rods, corresponding to $S \approx 0.55 \pm 0.02$, was measured at the highest achievable volume fractions of $\phi/\phi_{nem} \approx 1.35 \pm 0.09$. At the largest centrifugal field strengths, the volume fraction for all three aspect ratios studied converged to $\phi/\phi_{nem} \approx 1.25 \pm 0.07$. Comparison to previous theory and simulation of the isotropic–nematic transition of rod particles indicates that the field strengths required to generate nematic order were larger than would have been predicted under the assumption of local equilibrium in the sediments.

Introduction

Anisotropic colloidal particles are useful building blocks for assembly because they may self-organize into structures with symmetry more complex than the closely packed order typical of isotropic spheres.[1] Although two-dimensional assembly of anisotropic particles on surfaces and interfaces is of interest,[2–4] many applications such as optical materials require assemblies with high quality ordering in a three dimensional (3D) volume.[5] Among bulk, 3D colloidal phases that are targets for assembly from anisotropic building blocks, liquid crystal phases with orientational order are of particular interest. Statistical thermodynamics[6,7] predicts that an order–disorder transition in colloidal rods occurs as the consequence of a competition between translational and orientational contributions to the free energy. The volume fraction for nematic order, ϕ_{nem}, is a function of the aspect $r = L/D$ where L is the major-axis length of the rod and D is the minor axis diameter. The predicted coexistence range has been refined based on details of shape, as well for three-body interactions.[8] The implications of colloidal anisometry for equilibrium self-assembly have been addressed by experiment.[9]

Generation of orientational order by application of an external field is of fundamental interest because fields can significantly accelerate the kinetics of crystallization.[10] For small field strengths, field-assisted assembly is also directly connected to equilibrium self-assembly. In this case the external field is balanced by a spatial gradient in the ϕ-dependent osmotic pressure, $\frac{d\Pi(z)}{dz} = -\frac{mg}{V_p}\phi(z)$.[11] Here, $\Pi(z)$ is the osmotic pressure, m is the colloid buoyant mass, g is the gravitational constant, V_p is the volume of a rod particle, and $\phi(z)$ is the volume fraction of rods at a height z in the sediment. Thus, an external field, such as provided by gravity or centrifugation, will induce a spatially varying density field in a colloidal suspension. If the variation in colloid density induced by the field spans the boundaries of an equilibrium phase transition, then ordered assemblies are predicted.[12]

Although some examples of 3D field-assisted assembly have been reported, including the shear-induced assembly[13] of fd virus as well as the sedimentation of fd virus,[14] poly (methyl methacrylate),[15] and silica[16] rods, in these cases either disordered rod packings resulted, the onset of ordering was neither explained nor controlled, or the specimens were initially ordered prior to application of the field. Interesting orientation effects in the settling of concentrated suspensions have also been observed in experiments and simulations of non-Brownian fibers.[17–19] In this case a transition in the orientation distribution function with concentration has been linked to the role of inertia and finite Reynolds number (Re),[17] an effect that does not arise in the field-assisted assembly of micron-sized Brownian colloids, for which $Re < 1$. Yet, recent computer simulations suggest that order–disorder transitions ought to be accessible by field-assisted assembly[12,20] of Brownian rods provided that local equilibrium is achieved. On the other hand, simulations[21] and theory[22] suggest that kinetic effects and the rod glass transition could interfere with thermodynamically driven ordering transitions.

In this paper, we address the questions of whether field-assisted assembly can produce bulk nematic phases of anisotropic colloids, and if so, whether the variables that control the quality of orientational ordering can be identified. The field applied is the effective gravitational force induced by centrifugation. The quality of ordering in the assembled sediments is quantified by the nematic order parameter S,[12] where S is the largest eigenvalue of the orientation tensor $\boldsymbol{Q}$, where $\boldsymbol{Q} = \frac{1}{n_r}\left(\sum_{i=1}^{n_r}\frac{3\boldsymbol{u}_i\boldsymbol{u}_i - \boldsymbol{I}}{2}\right)$.

University of Michigan, Ann Arbor, MI, 48109-2136, USA. E-mail: mjsolo@umich.edu

Here, n_r is the number of rods in the specimen, $\boldsymbol{u}_i$ is the vector specifying the director of the i^{th} rod, and $\boldsymbol{I}$ is the identify matrix. This parameter is zero for a perfectly isotropic system and one for a perfectly aligned suspension. Here S is directly computed from $\boldsymbol{u}_i$ measured in 3D for individual rods by confocal microscopy. Although previous work[15] has computed a related 2D order parameter by direct visualization, the fully 3D calculation pursued here to analyze the confocal microscopy results is powerful because it allows direct comparison to previous results from simulation[23] and theory.[8]

Experimental section

Colloidal rod suspensions

The colloids are Brownian fluorescent rods comprised of poly(methyl methacrylate) that have been sterically stabilized by a surface layer of poly(dimethylsiloxane).[15,24] The particles were dispersed in a 62/38 (v/v) mixture of cyclohexyl bromide (CXB) and decalin (Sigma-Aldrich, USA), a mixture that is refractive index matched with the rods so as to allow confocal microscopy far into the sediment. At this ratio of CXB and decalin the solvent is approximately 6% less dense than the rods ($\Delta\rho \approx 0.068$ mg ml^{-1}).[25] Spheroids of aspect ratio 3.6 ± 0.2 (L and D of 2.8 (±0.11) and 0.78 (±0.03) μm, respectively), 5.0 ± 0.3 (L and D of 3.30 (±0.13) and 0.66 (±0.03) μm, respectively) and 8.0 ± 0.6 (L and D of 4.50 (±0.16) and 0.56 (±0.04) μm, respectively) were studied.

Centrifugation

Stable rod dispersions of an initial volume fraction, $\phi_{initial} = 0.02$, were subjected to the applied external field of centrifugation (AllegraTM 21R, Beckman Coulter, Inc., USA) in cylindrical glass vials of inner diameter (ID) 4 mm and height 1.5 cm. The orientation of the cell relative to the applied centrifugal field was typically as shown in Fig. 1a; however, the orientation of the container relative to the field did not significantly affect results. In a typical experiment the cell was completely filled (volume ≈ 200 μl) and centrifugation performed until a steady-state volume fraction profile, $\phi(z)$, was reached. The magnitude of the effective gravitational force ($g' = \omega^2 R$) was varied from 0.67g to 6700g by controlling the rotation rate ω of the centrifuge.

Confocal laser scanning microscopy (CLSM)

A confocal laser scanning microscope (Leica TCS SP2, Leica Microsystems Wetzlar, Germany) was used to acquire 3D image volumes of the sediment structure. Imaging was performed with a 100× oil immersion objective (numerical aperture 1.4). Except for experiments in which the volume fraction profile of the sediment was quantified (*cf.* Fig. 1C), a 3D image stack of approximate dimension 20 × 20 × 20 μm^3 was collected. The typical voxel size was 41 × 41 × 41 nm^3. In the frame of the microscope the centrifugation force was typically applied in a direction parallel to the objective plane.

Image processing codes, as described in ref. 15, were used to find, in 3D, the position and orientation of the central backbones of the rods in the specimen. The error in location is approximately 55 nm in the objective plane and 45 nm along the axis perpendicular to objective plane.[24] The error in the orientation of the rod director, $\boldsymbol{u}_i$, is greatest at lowest aspect ratio and never more than 0.25 radians.[24] Analysis of simulated rod image volumes indicated that the systematic error in $\boldsymbol{u}_i$ was less than 2%.

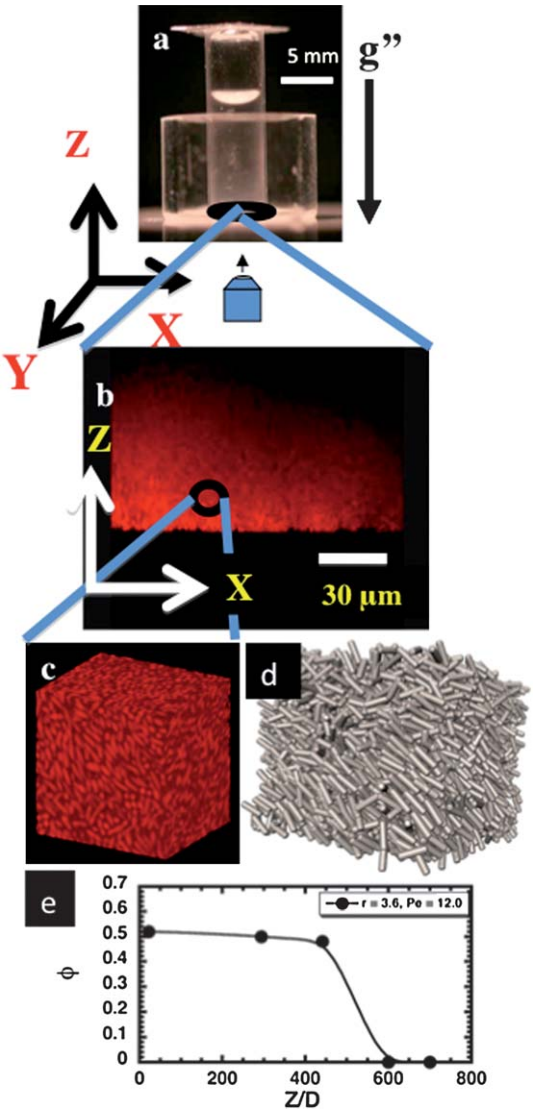

Fig. 1 (a) Design of the centrifugation cell and the direction of the effective gravitational field relative to it. (b) CLSM image of a sediment (2000 rpm, $r = 3.6$, $\phi_{initial} = 0.02$) in the plane parallel to the direction of gravitational field. (c) 2D projection of a 3D image volume collected for data analysis and (d) reconstruction of the image volume. (e) Dependence of final volume fraction on height from coverslip.

Results and discussion

The volume fraction of rods in the sediment is a maximum at the bottom of the container and thus the greatest potential for observing orientational order is in this region. Fig. 1b and e illustrate typical results at 2000 rpm for a suspension of rods of $r = 3.6$ and an initial volume fraction of 2%. The high concentration of rods persisted far into the sediment—about 400–600 rod diameters, before rapidly falling to zero at the sediment

boundary (Fig. 1e). We imaged specimens beginning at a height 10D and extending to as large as 220D, consistent with the densest regions of the sediment. Fig. 1c shows the two-dimensional projection of one of the three dimensional image stacks acquired for analysis of sediment structure. Fig. 1d is its reconstruction from image processing outputs of centroids and orientations. The initially homogeneous concentration of rods required time to respond to the effective gravitational force that was imposed by centrifugation. Time to steady state was assessed by measurements at 6, 12, 24 and 40 h (data not shown). The order parameter S of the sediments achieved steady-state conditions within 12 hours.

To report subsequent data, we use a dimensionless measure of the field strength. A number of closely related approaches are available. The first, reported by ref. 12 and 20, compares an effective length for the effect of gravity to the rod length, $\frac{\Delta\rho V_p g' L}{k_B T}$. Here g' is the effective gravitational acceleration, $\Delta\rho$ is the buoyant density, V_p is the particle volume, and L is rod length. The second approach, which we adopt here, compares the characteristic time scale for rotational diffusion to the time scale for free particle sedimentation the distance of a rod length. This quantity is the Peclet number, $Pe = \frac{\Delta\rho V_p g' L}{9k_B T}$. (Ref. 14 defines Pe based on the relative sedimentation velocity of two rods. In this case the numerical factor is 12 rather than 9. Shape dependent, order one factors of $\ln(r)$ have been suppressed in writing this definition of Pe.[26]) For this study, $0.03 < Pe < 400$.

Confocal microscopy images that report the qualitative effect of centrifugation on ordering are shown in Fig. 2 for rods of aspect ratios $r = 3.6$ (Fig. 2a–c) and $r = 8.0$ (Fig. 2d–f). The corresponding values of Pe vary from 0.03 to 400. The images show qualitative effects of the applied field on ordering. For $r = 3.6$, an increase is observed in both volume fraction and ordering with increasing centrifugal force. We note that although only 2D images are shown, rods were also aligned in 3D across the full image volume which was of dimension ~10 rod lengths. Image processing showed that the maximum volume fraction of rods for $r = 3.6$ was $\phi = 0.58$ (at $Pe = 300$). For $r = 8.0$, the maximum volume fraction achieved was $\phi = 0.43$ (at $Pe = 0.4$).

In Fig. 3, we plot the dependence of the nematic order parameter S, the largest eigenvalue of the orientation tensor $\boldsymbol{Q}$, on the dimensionless field magnitude Pe. Error bars are standard error of the mean assessed by three replications at a number of the Pe studied. For $r = 3.6$, the value of S increases from 0.12 to 0.56 when the effective gravitational field is increased from $0.67g$ to $6700g$ (over the span of two decades of Peclet number), consistent with the images of Fig. 2a–c. The plot shows a similar increase of S with Pe observed for $r = 5$ rods. However, a very different Pe dependence was observed for $r = 8$ rods. In this case a strong centrifugal field had adverse effects on ordering. That is, at low Pe and $r = 8$, rod densification did occur upon centrifugation. However, as Pe was increased, orientational ordering progressively deteriorated. Thus, Fig. 3 shows that aspect ratio had a qualitative effect on the orientational order induced by an applied field.

Two hypotheses might explain the complex trends in S plotted in Fig. 3. The first explains the ordering as the consequence of equilibrium phase transitions induced by the concentrating effect of the applied field.[6,8] Indeed for hard rods in local equilibrium, the isotropic–nematic transition is purely a function of the local sediment volume fraction, $\phi(z)$. As per,[14] application of such an equilibrium theory to the field-assisted assembly process of sedimentation requires $Pe < 1$. For the $r = 3.6$ measurements

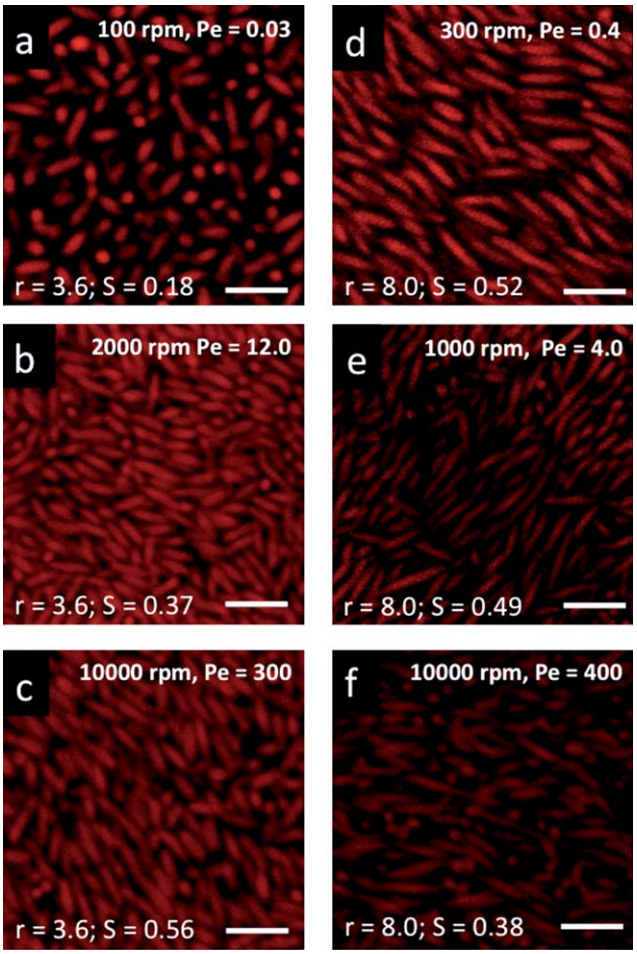

Fig. 2 2D images of CLSM image volumes of colloidal sediments made under different gravitational fields for the rods of aspect ratio 3.6 (a–c), in the order of increasing centrifugal field (Pe), and also for $r = 8.0$ (d–f), also in the order of increasing centrifugal field. Scale bars in the images are 4 μm.

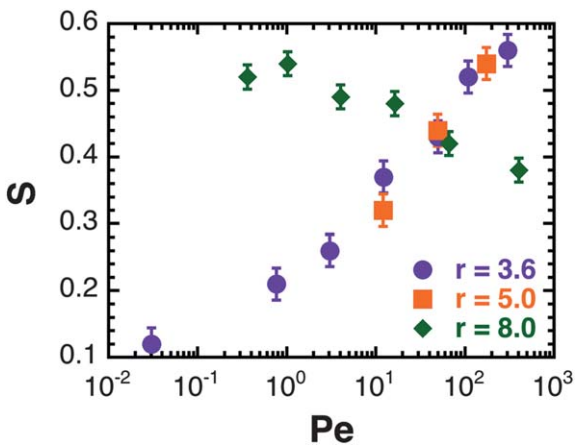

Fig. 3 Dependence of nematic order parameter S on the Peclet number, Pe, for rods of aspect ratios 3.6, 5.0 and 8.0.

reported in Fig. 3, this criterion is met for only one of the measurement conditions.

The second hypothesis explains the ordering in Fig. 3 as a non-equilibrium effect of the applied field. The observation that $Pe > 1$ is required for the most significant ordering to occur would favor a role for this hypothesis. An example of a non-equilibrium effect would be a preferred rod orientation induced by the applied field at low volume fraction, in the initial stages of sedimentation, which is subsequently perpetuated by the slowing down of rotational diffusion induced by the high rod volume fraction at later times.[18] Such an effect, dependent on the time varying balance between field-induced alignment and orientational disorder induced by rotational diffusion, would be controlled by the magnitude of the Pe number.

Although both hypotheses are plausible, Fig. 3 alone does not provide information sufficient to distinguish between them. If the equilibrium I–N transition plays a role, the ordering ought to correlate with the local sediment volume fraction, ϕ, scaled on the aspect ratio dependent volume fraction of the nematic phase, ϕ_{nem}. Image processing of the sediment CLSM volumes yields ϕ as a function of Pe. ϕ_{nem} for the three different aspect ratios was taken from the results of ref. 8 for ellipsoids. Results are plotted in Fig. 4. Although the Pe dependence of orientational ordering in these suspensions differs significantly (recall Fig. 3), the quality of ordering, as quantified by S, is well correlated by the control parameter ϕ/ϕ_{nem}, as shown in Fig. 4. (That is, by comparing Fig. 3 and 4, we see that S is better correlated by ϕ/ϕ_{nem} than by Pe.) This correlation supports the idea that the equilibrium isotropic–nematic transition is predictive of orientational order in the field-assisted assembly process of centrifugation. From the point of view of applications, this connection provides a systematic way to utilize centrifugation so as to achieve large scale, 3D orientational ordering in colloidal rod suspensions. That is, if an effective centrifugal field strength (as parameterized by Pe) can be designed so that $\phi/\phi_{nem} > 1$ results, then orientational ordering of the rods would result.

In Fig. 4, we also plot the equilibrium theoretical predictions of S for ellipsoids of aspect ratio 3, 5 and 10 as taken from ref. 8. The theory predicts a transition to a finite S at $\phi/\phi_{nem} \approx 1$. As discussed above, the increase in S found in the experiments occurs as $\phi/\phi_{nem} \approx 1$ as well, so the equilibrium order–disorder transition has some role to play in field-assisted assembly, even in the $Pe > 1$ regime of these experiments. Yet, substantive differences between the equilibrium theory and the field-assisted experiment are apparent. First, the magnitudes of the measured order parameters are significantly less than the equilibrium theory. For example, at $\phi/\phi_{nem} \approx 1.2$, the theory is shifted upward from the experiment by about 50%. (In comparison, the order parameter in concentrated solutions of filamentous virus from scattering has been reported to be $S = 0.55$.[27] Deviations in this case from the hard rod result were attributed to the finite flexibility of the fd virus. Nematic texture, if the nematic structure was not monodomain over the region of analysis, could also result in a reduction in S relative to theory.) Second, while theory predicts an abrupt increase in S at $\phi/\phi_{nem} \approx 1$, a more gradual transition is observed for the experimental measurements. Third, the concavity of the dependence of S on ϕ/ϕ_{nem} differs—the theory is concave downward, the experiments are concave upward. Fourth, the experiments show a finite S for $\phi/\phi_{nem} < 1$, a region for which the equilibrium theory predicts $S = 0$. These four differences between the theory of ref. 8 and the experiments of this work suggest that non-equilibrium effects are indeed important in field-assisted assembly in the Pe number range studied.

Notwithstanding such non-equilibrium effects, it still remains that the primary effect of the field on orientational ordering is to densify the sediments and that densification to $\phi \approx \phi_{nem}$ is predictive of a finite order parameter in the suspensions. In Fig. 5, we further examine this effect by plotting ϕ/ϕ_{nem} *vs.* Pe for all the aspect ratios studied. The plot shows that for $Pe < 10$ the dependence of volume fraction on Pe for long aspect ratio rods ($r = 8.0$) is very different from low aspect ratio rods of 3.6 and 5.0. However, for $Pe > \sim 10^2$, the results for the different

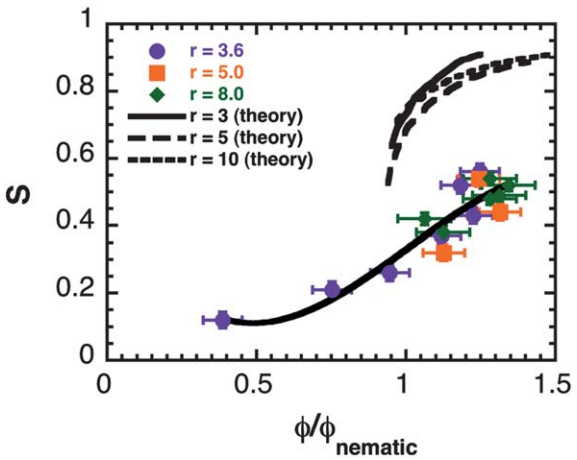

Fig. 4 Dependence of nematic order parameter S on the volume fraction at the base of the centrifuge cell, scaled on the aspect ratio dependent ϕ_{nem}, for the rods of aspect ratio 3.6, 5.0 and 8.0. Values of ϕ_{nem} were estimated from ref. 8 to be 0.465, 0.426 and 0.320 for $r = 3.6$, 5.0, 8.0, respectively. Theoretical curves are replotted from the figures of ref. 8 for $r = 3$, 5 and 10.

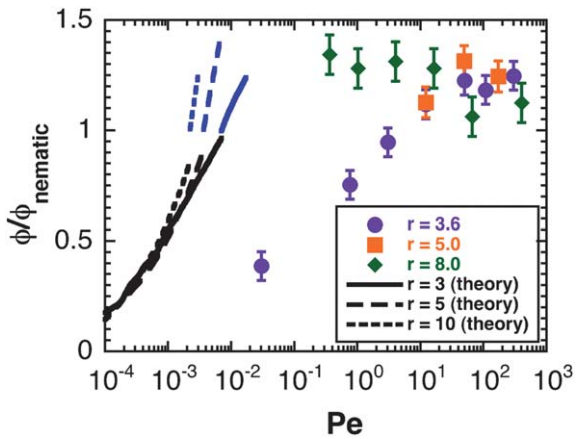

Fig. 5 Dependence of scaled volume fraction, ϕ/ϕ_{nem} on the Peclet number for the rods of aspect ratios 3.6, 5.0 and 8.0. Theoretical curves are computed from the volume fraction dependent osmotic pressure for $r = 3$, 5 and 10 as reported in ref. 8. The curves plotted are for the case of $V_p = 0.75\ \mu m^3$ and a cell geometry and initial volume fraction that match those of the experiments.

aspect ratio rods approximately converge to a plateau of magnitude $\sim 1.25 \pm 0.07$ times ϕ_{nem}.

The connection between the applied field strength and the ϕ-dependent osmotic pressure, $\frac{d\Pi(z)}{dz} = -\frac{mg}{V_p}\phi(z)$, valid for small Pe, would predict a monotonically increasing effect of Pe on ϕ/ϕ_{nem} in Fig. 5. We generated these predictions from the theoretical equation-of-state results for $r = 3$, 5 and 10 ellipsoids available in ref. 8. These curves are also plotted in Fig. 5. Comparing the equilibrium predictions to the field-assisted assembly results shows that the experiments at $r = 3.6$ and 5 require much larger Pe to achieve the high volume fractions necessary for ordering than the equilibrium theory would suggest. Furthermore, at these high Pe, all three aspect ratios tend to a limiting volume fraction that is approximately a constant multiple of the nematic phase transition volume fraction, $\sim 1.25^*\phi_{nem}$. Indeed, for $r = 8$, it is necessary to operate at an intermediate Pe ($Pe \approx 10^1$ or less) to achieve the highest volume fractions ($\sim 1.35 \pm 0.09^*\phi_{nem}$) that yield the greatest ordering.

We conclude by discussing four implications of the comparison between the theory of field-assisted assembly, which implicitly assumes local equilibrium,[14] and the experimental observations.

First, from Fig. 5, much larger dimensionless applied field strengths (Pe) were required to generate orientational order by centrifugation than the simple equilibrium theory of $\frac{d\Pi(z)}{dz} = -\frac{mg}{V_p}\phi(z)$ would imply. For example, for $r = 3.6$ and $Pe \approx 0.03$, the equilibrium theory would suggest that the sediment volume fraction should be above the nematic transition ($\phi/\phi_{nem} \approx 1.2$, Fig. 5) and the specimen fully ordered ($S > 0.8$, Fig. 4). Instead, the experiments show incomplete densification ($\phi/\phi_{nem} < 0.5$) and negligible ordering ($S < 0.15$) at this aspect ratio.

Second, as discussed in ref. 14, the local equilibrium assumption that a rod samples its rotational distribution function within the time required to sediment its length breaks down for $Pe > 1$. Yet, even given the dominance of the applied field in this regime, the equilibrium nematic transition volume fraction remains the variable that best predicts the degree of orientational order of the specimen. That is, if Pe is such that $\phi/\phi_{nem} > 1$, then orientational order, as quantified by S, is observed.

Third, the field-assisted assembly theory described here, which is valid for $Pe < 1$, does not prescribe a particular orientation of the nematic structure which results due to field-induced densification. As assessed from the image volumes and additional, lower-resolution imaging performed, the centrifugal assembly method largely yielded monodomain nematic structure in the $20 \times 20 \times 20\ \mu m^3$ regions (~ 5000 rod particles) that were visualized. We did find that the azimuthal orientation of the nematic structure (where this angle is defined in the plane parallel to the bottom surface of the container) was randomly distributed over the experiments. However, the nematic director of the sediments did appear biased toward a polar angle orientation that was consistent with rods lying preferentially in a plane parallel to the bottom surface. This bias suggests some effect of the bottom surface on the nematic orientation, an effect not included in the theory. Another possible effect is the orientation dependent drag coefficient of ellipsoids,[28] which could interact with the field direction to produce bias toward particular nematic directions.

Finally, the observation of the limiting volume fraction behavior $\phi \approx 1.25\phi_{nem}$ for $Pe > \sim 10^2$ is unexpected. At this condition, since $S \approx 0.5$ (Fig. 4), it is interesting to consider the possibility of a glass or jamming transition of the nematic liquid crystal. In this case, the observed assemblies would be consistent with the frozen nematic texture and oriented glass or gel structures discussed, for example, in ref. 29 and 30.

Conclusion

In this study we have identified how the strength of an applied field, in this case the centrifugal force, can be controlled so as to generate colloidal liquid crystals of rods with finite order parameter, S. The summary of this study's findingsis: (i) the local sediment volume fraction achieved by the applied field determines the quality of orientational order as quantified by the order parameter, S; (ii) The onset of significant orientational ordering correlates well with the equilibrium nematic volume fraction, ϕ_{nem}; (iii) The maximum rod order parameter ($S \approx 0.55$) is found at the highest achievable local volume fractions (Fig. 3); (iv) The three aspect ratios studied converge to a limiting volume fraction of $1.25^*\phi_{nem}$ at the highest Pe studied, $Pe \approx 10^2$. Comparison to the predictions for field-assisted assembly valid under conditions of local equilibrium[12] and computed from equation-of-state information[8] suggests that the local equilibrium hypothesis is insufficient to describe the observed orientation effects. These experiments can thus motivate the future development of approaches that incorporate the effects of field on nematic orientation, including the particular direction of the nematic texture, and thus better describe the regime of $Pe > 1$ in which nematic order of the rod colloids was observed. The results also provide a systematic method to achieve rapid, bulk nematic order in colloidal rods by the application of an applied field.

Acknowledgements

This study was supported by the National Science Foundation (NSF CBET 0707383).

References

1 S. C. Glotzer and M. J. Solomon, *Nat. Mater.*, 2007, **6**, 557–562.
2 B. Madivala, J. Fransaer and J. Vermant, *Langmuir*, 2009, **25**, 2718–2728.
3 S. P. Wargacki, B. Pate and R. A. Vaia, *Langmuir*, 2008, **24**, 5439–5444.
4 J. P. Singh, P. P. Lele, F. Nettesheim, N. J. Wagner and E. M. Furst, *Phys. Rev. E: Stat., Nonlinear, Soft Matter Phys.*, 2009, **79**, 050401.
5 V. L. Colvin, *MRS Bull.*, 2001, **26**, 637–641.
6 L. Onsager, *Ann. N. Y. Acad. Sci.*, 1949, **51**, 627–659.
7 G. J. Vroege and H. N. W. Lekkerkerker, *Rep. Prog. Phys.*, 1992, **55**, 1241–1309.
8 B. Tjiptomargo and G. T. Evans, *J. Chem. Phys.*, 1990, **93**, 4254–4265.
9 Z. Dogic and S. Fraden, *Curr. Opin. Colloid Interface Sci.*, 2006, **11**, 47–55.
10 J. Vermant and M. J. Solomon, *J. Phys.: Condens. Matter*, 2005, **17**, R1–R30.
11 W. B. Russel, D. A. Saville and W. R. Schowalter, *Colloidal Dispersions*, Cambridge University Press, Cambridge, 1989.

12 S. V. Savenko and M. Dijkstra, *Phys. Rev. E: Stat., Nonlinear, Soft Matter Phys.*, 2004, **70**, 051401.
13 M. Ripoll, P. Holmqvist, R. G. Winkler, G. Gompper, J. K. G. Dhont and M. P. Lettinga, *Phys. Rev. Lett.*, 2008, **101**, 168302.
14 Z. Dogic, A. P. Philipse, S. Fraden and J. K. G. Dhont, *J. Chem. Phys.*, 2000, **113**, 8368–8380.
15 A. Mohraz and M. J. Solomon, *Langmuir*, 2005, **21**, 5298–5306.
16 S. Sacanna, L. Rossi, A. Wouterse and A. P. Philipse, *J. Phys.: Condens. Matter*, 2007, **19**, 376108.
17 E. Kuusela, J. M. Lahtinen and T. Ala-Nissila, *Phys. Rev. Lett.*, 2003, **90**, 094502.
18 B. Metzger, J. E. Butler and E. Guazzelli, *J. Fluid Mech.*, 2007, **575**, 307–332.
19 B. Herzhaft and E. Guazzelli, *J. Fluid Mech.*, 1999, **384**, 133–158.
20 V. A. Baulin and A. R. Khokhlov, *Phys. Rev. E: Stat., Nonlinear, Soft Matter Phys.*, 1999, **60**, 2973–2977.
21 T. A. Schilling and D. Frenkel, *Comput. Phys. Commun.*, 2005, **169**, 117–121.
22 G. Yatsenko and K. S. Schweizer, *Langmuir*, 2008, **24**, 7474–7484.
23 D. Frenkel and B. M. Mulder, *Mol. Phys.*, 1985, **55**, 1171–1192.
24 D. Mukhija and M. J. Solomon, *J. Colloid Interface Sci.*, 2007, **314**, 98–106.
25 R. E. Rogers, Assembly of Colloidal Crystals with Well-characterized Pair Interaction Potentials, PhD thesis, University of Michigan, 2010.
26 M. Doi and S. F. Edwards, *The Theory of Polymer Dynamics*, Clarendon Press, Oxford, 1986.
27 K. R. Purdy, Z. Dogic, S. Fraden, A. Ruhm, L. Lurio and S. G. J. Mochrie, *Phys. Rev. E: Stat. Nonlinear Soft Matter Phys.*, 2003, **67**, 031708.
28 L. G. Leal, *Laminar Flow and Convective Transport Processes*, Butterworth-Heinemann, Boston, 1992, p 246.
29 J. Buitenhuis and A. P. Philipse, *J. Colloid Interface Sci.*, 1995, **176**, 272–276.
30 Z. K. Zhang, N. Krishna, M. P. Lettinga, J. Vermant and E. Grelet, *Langmuir*, 2009, **25**, 2437–2442.